Journal of *Fungi*

MDPI

Article

The Fungal, Nutritional, and Metabolomic Diagnostics of the Oil Palm *Elaeis guineensis* Affected by Bud Rot Disease in Esmeraldas, Ecuador

Raluca A. Mihai [1,*], Erly J. Melo Heras [2], Pablo A. Landazuri Abarca [2] and Rodica D. Catana [3]

[1] CICTE, Department of Life Science and Agriculture, Universidad De Las Fuerzas Armadas—ESPE, Av. General Rumiñahui s/n y Ambato, Sangolquí 171103, Ecuador
[2] Department of Life Science and Agriculture, Universidad De Las Fuerzas Armadas—ESPE, Av. General Rumiñahui s/n y, Sangolquí 171103, Ecuador; ejmelo@espe.edu.ec (E.J.M.H.)
[3] Institute of Biology Bucharest, Romanian Academy, 060031 Bucharest, Romania
* Correspondence: rmihai@espe.edu.ec

Abstract: The oil palm *Elaeis guineensis* represents one of the most important crops in Ecuador. Considering that bud rot disease is deadly in Ecuador, more attention has been given to identifying possible causes for palm debility from this disease. We studied the involvement of fungi and nutrients in triggering bud rot disease in *E. guineensis.* Special emphasis was given to the molecules synthesized by the plant to protect against this devastating disease. Techniques like Diagnosis and Recommendation Integrated System (DRIS) and metagenomic analysis were used to understand the possible implications of biotic and abiotic factors in the development of bud rot disease in oil palm in Ecuador. Liquid chromatography-mass spectrometry (LC-MS) analysis was used to identify the phenolic protection barrier of the palm facing the disease. Our results indicate that fungi from *Ascomyceta* phylum were found in the tested samples. The species directly involved are different in soil compared with plants. The results indicate a deficiency of chemical elements, such as Ca, Mn, Mg, and Fe, which are responsible for palm debility from bud rot disease. More than 30 compounds with protective roles were identified in the leaves of symptomatic plants from the first stage of the infection.

Keywords: fungi; bud rot; nutrition status; palm oil; 16S; metabolomics; DRIS; HPLC-MS

Citation: Mihai, R.A.; Melo Heras, E.J.; Landazuri Abarca, P.A.; Catana, R.D. The Fungal, Nutritional, and Metabolomic Diagnostics of the Oil Palm *Elaeis guineensis* Affected by Bud Rot Disease in Esmeraldas, Ecuador. *J. Fungi* **2023**, *9*, 952. https://doi.org/10.3390/jof9090952

Academic Editor: Xiaohui Pang

Received: 27 July 2023
Revised: 1 September 2023
Accepted: 12 September 2023
Published: 21 September 2023

1. Introduction

Elaeis guineensis, the African oil palm native to West Africa, is the most important palm species, being the world's highest-yielding edible oil crop used in the food and nonfood sectors [1]. The interest in *E. guineensis* is given by its economic importance because it is the world's largest edible oil [2] with numerous medicinal values [3].

At the global level, palm oil crops are dealing with numerous pressures [4], like pathogens represented by fungi, bacteria, viroids, and viruses [5], which are affecting the oil palm by reducing yield or retarding growth [6]. At various times, oil palm plantations from southeast Asia, Africa, and South America were affected by almost 32 diseases and disorders [7]. Among diseases, bud rot is a catastrophic one affecting more than 50% of the plantations [8]. Bud rot is one of the two important phytosanitary problems in tropical America.

But rot destroys the young tissue of the plants; the lesions appear to descend from the middle of unopened internal leaves to the meristematic zone followed by chlorosis of the youngest leaves, necrosis, and plant death [9]. Once the lesions progress, colonization with pathogens occurs [10]. Until now, two forms of bud rot disease have been found: a lethal one (in Ecuador, Brazil, Colombia, and Suriname) and a nonlethal form with a good recovery rate (in Colombian Llanos) [11]. The highest incidence in Ecuador is in the

coastal areas, especially in the province of Esmeraldas, where the temperature and relative humidity are naturally favorable for this disease's high incidence and spread. Starting in the 2020s, bud rot has been the main cause of deterioration and loss of plantations in Ecuador.

In 2020, Ecuador was the 17th largest producer worldwide of oil palm and the 15th largest exporter in the world [12] due to its growing and stable culture. Ecuador has 200,908 hectares (496,454 acres) of oil palm plantations, 40% in Esmeraldas, 18.5% in Los Ríos, and 10% in Santo Domingo. Esmeraldas is characterized by the highest rate of deforestation in the country and also by the largest oil palm plantations in Ecuador according to the National Institute of Statistics and Census, 2019 [13].

Even if bud rot symptoms are easy to recognize, diagnostic confirmation is difficult due to the pathogen's colonization, which makes it difficult to identify the agents and therefore the possibility of applying a treatment [9]. Two types of factors were identified for this disease: biotic and abiotic factors. At the international level, bacteria *(Erwinia* spp.) [14], fungi (*Thielaviopsis* spp. and *Fusarium* spp.) [15], and Oomycetes *(Pythium* spp. and *Phytophthora* spp.) [10] were identified as being the organisms involved in bud rot disease. The nutrition status may represent the abiotic factor [16,17]. An improper level of minerals might trigger susceptibility to beneficial microorganisms. In this context, there is a lack of studies on the nutritional factors affecting bud rot disease in Ecuador.

Successful disease management consists in the use of resistant planting material [18], proper drainage, good fertilization, intense monitoring, and rapid agronomic interventions (destruction of infected palms) [19]. Before establishing a new plantation, farmers are advised to improve their drainage systems and to analyze the soil's biodiversity [20].

An important factor in plant development is played by the rhizosphere microbiome [21]. The studies concerning the association between *E. guineensis* and microbial communities were focused on the use of bacteria isolated from the rhizosphere to promote plant growth or control the white rot fungus *Ganoderma boninense* [22].

MiSeq sequencing is a molecular technique that detects and identifies fungal and bacterial species from different samples, like plants, food, water, and soil [23].

Secondary metabolites represent the molecules identified in different aspects of the plant. One of the major roles of these molecules is plant protection against different types of stress, such as biotic (bacteria, fungi, nematodes, and insects) and abiotic (temperature, moisture, shading, heavy metals, and different levels of nutrients) [24].

This investigation is the first one that tries to demonstrate the biotic (fungi) and abiotic (nutritional involvement) factors involved in bud rot disease development in the oil palm plantations from the Esmeraldas area. Also, important aspects concerning the secondary metabolites in the symptomatic plants were investigated.

2. Materials and Methods

2.1. Study Area

Ecuador has 8149 oil palm plantations, and the province of Esmeraldas is the one with the highest production with 3280 plantations and 116,430.38 hectares, while Quinindé Canton represents 37% of plantations at the national level and 91% at the provincial level [25]. The Canton is located 100 km from the Province of Esmeraldas, to the southeast of its territory, at 00°13′33″ N Latitude, 73°26′00″ W Longitude, and it has an average height of 115 m.a.s.l., a 21–31 °C temperature range, and an average annual precipitation of 2300 mm, except for abnormal periods, such as the El Niño phenomenon [26]. The environmental climatic conditions are represented by relatively mild temperatures in winter, a warm summer, and rainfall distributed throughout the year. The dominant coverage of the study area is 52.2% forest and 44.8% agriculture [27].

The soil in the study area (78% medium-high fertility soil and 22% low-fertility soil) is represented by sediments from the ancient plains and mountain ranges of the coastal region, with a greater amount of water per volume of soil, greater retention of ions in interchangeable form, and greater resistance to leaching processes [28].

2.2. Foliar Sample Collection

The plant material was represented by the middle part of leaf number 17 of the oil palm *Elaeis guineensis* Jacq. adult plants collected from three plantations, in Ecuador, in July 2022, a period of low rainfall, and no fertilization, which may reduce the variability of the results. The harvested leaflets were cleaned before drying (at 70 °C), ground in a stainless-steel Wiley mill, and analyzed for total N by micro-Kjeldahl. An atomic absorption spectrophotometry was used for K, Ca, Mg, Fe, Zn, and Cu. A colorimetric method using vanadate molybdate reaction was used to detect phosphorus, a turbidimetric method for boron, and a photometry method for sulfur. Our results expressed in % (macronutrients) and mg/kg (micronutrients) were compared with the standards developed by Marrocos et al. (2020) [29].

2.3. Soil Sample Collection

The soil samples were collected in the morning hours, from the same palm sample used for the foliar analysis, consisting of 10 cores to a depth of 30 cm, and transported in plastic bags disposed of in cooler recipients to the laboratory for further analysis of pH, phosphorus (P), calcium (K), calcium (Ca), and magnesium (Mg) using the standard procedures of the Belle Glade, AREC—Agricultural Research and Education Center. For the determination of soil pH used in a 1:2 soil–water suspension, an AI block with nitric and perchloric acids was used to digest the ground sample [30]. Total P was determined by the molybdovanadophosphate colorimetric procedure [31] and K, Ca, Mg, Fe, Mn, Zn, and Cu were determined by atomic absorption spectrophotometry.

2.4. DRIS Analysis

The DRIS (Diagnosis and Recommendation Integrated System) method uses "nutrient ratios" instead of absolute or individual nutrient concentrations for the interpretation of tissue analysis. The use of leaf nutritional assessment based on DRIS, in addition to the traditional methods such as the levels of critical ranges, is an important tool that mitigates the distortions of diagnoses caused by the effect of dilution, concentration, age, or plant organ [32]. To carry out the DRIS, an average of the foliar analyses was calculated to have a global reference for the area under study. Once the DRIS indices were obtained, the IBNM (analysis of nocturnal basal impedance) was obtained based on the formula:

$$\mathrm{IBNa} = \frac{\mathrm{IA} + \mathrm{IB} + \mathrm{IC} + \cdots \mathrm{IN}}{\mathrm{Z}} \quad (1)$$

where IBN—the nutritional balance index, I—index, a—average, and Z—the number of indexes analyzed.

The IBNa with the standard deviation of the indices allows us to obtain the Potential Responses to the Application of Nutrients (RAPNs) [33]. The methodology used for the Potential Response to the Application of Nutrients was described by De La Torre, 2012 [33], where the absolute value of Ix was taken and transformed to ln, since IBMa and Ix are distributed exponentially according to their dry mass. RAPNs were obtained by subtracting the Ln/lx from Ln/IBMa| for each of the indices and to obtain the limits, SD|IBNa| (standard deviation) the upper and lower limits according to this definite integral (Table 1). According to Beaufils, 1973 [34], the sum of the DRIS indices is constrained to zero.

$$\int_{\alpha}^{\beta} \frac{1}{\sigma\sqrt{2\pi}} e^{\frac{[(Ix)i - IBNa]2}{2a2}} dx \quad (2)$$

Table 1. The Potential Response to the Application of Nutrients (RAPN) categories.

Potential Response to the Application of Nutrients (RPAN)	Inferior Limit (α)	Superior Limit
Cryodeficiency	$-\infty$	$-\frac{4}{3}\sigma$
Prone to Deficiency	$-\frac{4}{3}\sigma$	$-\frac{2}{3}\sigma$
Nutritional Balance	$-\frac{2}{3}\sigma$	$\frac{2}{3}\sigma$
Prone to Excess or Toxicity	$\frac{2}{3}\sigma$	$\frac{4}{3}\sigma$
Excess or Toxicity	$\frac{4}{3}\sigma$	∞

2.5. Metagenomic Analysis

Samples used for metagenomics were represented by soil (S1 and S2) and leaves (S3 and S4) collected from an *E. guineensis* plantation older than 4 years old. The soil samples were collected around the symptomatic plants (in stage 1) (S1) and healthy plants (S2). The plant samples were represented by symptomatic plants (in stage 1) (S3) and healthy plants (S4). The analysis was performed by BioSequence Ecuador.

For the extraction of fungal genome DNA, leaves were collected after the previous identification of the disease stage, placed in aseptic bags, and kept at low temperatures to prevent senescence while being transported to the laboratory. Leaf samples from each plant were disinfected by applying a series of washing steps, as mentioned by Badotti et al., 2017 [35], which consisted of 70% (v/v) ethanol for 1 min, 3% (v/v) sodium hypochlorite solution for 3 min, 2.5% (w/v) sodium thiosulfate for 5 min, and rinsing the samples five times with sterile water.

2.5.1. DNA Extraction

For DNA extraction, leaf samples were ground into a fine powder by using liquid nitrogen in a sterilized mortar and transferred into a bead tube for total DNA extraction. For subsequent analysis, DNA was stored at −20 °C. Target-specific primers were chosen from the MiSeq Illumina platform according to recommendations for fungal metabarcoding (Table 2), using indexes from the Nextera XT Index Kit v2 (Illumina, Catalog No. FC-131-2001).

Table 2. The ITS1 primer sequences were used for the analysis of the sample.

Primer Sequence for ITS1 Region	
Forward	ITS_fwd_1 CTTGGTCATTTAGAGGAAGTAA ITS_fwd_2 CTCGGTCATTTAGAGGAAGTAA ITS_fwd_3 CTTGGTCATTTAGAGGAACTAA ITS_fwd_4 CCCGGTCATTTAGAGGAAGTAA ITS_fwd_5 CTAGGCTATTTAGAGGAAGTAA
Reverse	ITS_rev_1 GCTGCGTTCTTCATCGATGC ITS_rev_2 GCTGCGTTCTTCATCGATGG ITS_rev_3 GCTACGTTCTTCATCGATGC ITS_rev_4 GCTGCGTTCTTCATCGATGT ITS_rev_5 ACTGTGTTCTTCATCGATGT

The PCR amplification was performed according to Siddique et al., 2022 [36] for a 25 µL PCR mixture, which consisted of 1X Dream Taq buffer, 0.16 µM dNTP mix, 0.4 µM forward and reverses primers, 0.25 µg template DNA and 0.75 unit Dream Taq DNA polymerase and PCR grade water. The PCR reaction was conducted as described by Al-Bulushi et al., 2017 [37] with the next settings: an initial denaturation step of 95 °C for 5 min, 25 cycles of denaturation at 94 °C for 30 s followed by an annealing step at 54 °C for 40 s and extension step at 72 °C for 1 min, final extension 10 min at 72 °C.

2.5.2. MiSeq Illumina Sequencing

For the sequencing, the method described by Hoggard et al., 2018 [38] was followed. A purification step was conducted for the initial PCR reaction using an Axygen PCR cleanup kit (Axygen), and then the quality was verified with 1% Thermo Fischer Scientific Massachusetts, U.S. agarose gel electrophoresis. The purified solution was diluted; then, it was used in a range of 50 to 100-fold as a new template for a second PCR under similar conditions to the first PCR, except for using 10 cycles as recommended by Al-Sadi and Kazerooni, 2018 [39]. For this PCR round, the Illumina Nextera PCR primers described in Table 3 were used, which were followed by quantification with a Quantus® by Promega (Promega, Quito, Ecuador)). Amplicons were pooled and submitted for sequencing using an Illumina MiSeq (Illumina, Inc., San Diego, CA, USA).

Table 3. Nextera adapter sequences.

	Overhang Adapter Sequences
Forward	TCGTCGGCAGCGTCAGATGTGTATAAGAGACAG-CTTGGTCATTTAGAGGAAGTAA
Reverse	GTCTCGTGGGCTCGGAGATGTGTATAAGAGACAG-GCTGCGTTCTTCATCGATGC

Adapted from Hoggard et al., 2018 [38].

2.6. Bioinformatics and Data Analysis

Adapters can pose a problem for library preparation on Illumina (FASTQ), so Trimmomatic is used to trim Illumina data (FASTQ) and remove adapters. The PAIRED END mode will keep read pairs matched and will also use the additional information contained in the paired reads to better find the adapter or PCR primer fragments introduced by the library preparation process [40]. FLASH (Galaxy Version 1.2.11.4) software was used to splice the reads of each sample; then, data were processed with the Trimmomatic (Galaxy Version 0.38.1) software to filter the spliced raw tags to obtain high-quality tags as described by Fan et al., 2020 [41]. Subsequently, identification at the species level was conducted through BLAST+ after downloading the UNITE database v8.2 [42,43].

2.7. LC-MS

2.7.1. Extraction Process

Plant material (leaves from symptomatic plants—in stage 1) was dried by lyophilization at −57 °C and 0.50 hPa for 48 h before extraction and stored at 4 °C in plastic tubes. Dried and ground solid residue samples (1 g) were extracted with 20 mL of 80% methanol for 2 h at 30 °C as recommended by Irakli et al. (2021) [44]. The extract was centrifuged at 5000 rpm for 10 min at 4 °C (Eppendorf 5490 centrifuge, Hamburg, Germany); then, it was filtered and concentrated with a rotary evaporator (Buchi, New Castle, DE, USA). The concentrated extract was stored at −20 °C until analysis.

2.7.2. LC-MS Analysis

Dry filtrates were diluted to 1000 mg/L and filtered with a 0.47 µm microfiber filter before LC-MS analysis. The injection volume was 5 µL through an Accucore Vanquish 150 × 2.1 mm column. The mobile phase consisted of 0.1% formic acid in water (v/v) (Solvent A) and acetonitrile (Solvent B) with a mobile phase flow rate of 0.5 mL/min, as described by Kang et al. (2016) [45]. The phenolic compounds were identified with accurate retention time, according to the mobile phases used by Bikoro Bi Athomo et al., 2021 [46].

3. Results

3.1. DRIS Analysis Based on the Soil and Foliar Determinations

Table 4 and Figure 1 present the DRIS indexes of nutrients to serve as a guide to quickly diagnose the nutrients needed by the palm which can influence its response in front of pathogens, making it resistant or feeble.

Table 4. DRIS indexes and Response to Nutrient Application Potential (RPANs) for oil palm culture (IN, IK, IP, ICa, IMg, IS, IB, IFe, IMn, IZn, and ICu) in palms affected by the bud rot disease.

DRIS Index/IBN	Healthy Plants		Bud Rot Disease Infection Stages in Oil Palm Stage I		Stage II		Stage III	
	Indices	RPANs	Indices	RPANs	Indices	RPANs	Indices	RPANs
IN	−396.74	−0.0	−411.27	−0.02	−517.24	−0.03	−500.30	−0.06
IP	−622.36	−0.44	−468.81	−0.15	−513.36	−0.02	−567.44	−0.18
IK	347.43	0.14	571.37	0.35	1012.20	0.70	774.99	0.50
Ica	−266.58	−0.41	−274.21	−0.39	−360.95	−0.33	−246.98	−0.65
IMg	−343.01	−0.15	−327.64	−0.21	−345.97	−0.37	−411.53	−0.14
IS	−414.41	−0.04	−350.33	−0.14	−391.10	−0.25	−430.52	−0.09
IB	175.26	0.82	204.91	0.68	271.70	0.61	295.41	0.47
ICu	451.92	0.12	367.41	0.09	349.42	0.36	432.07	0.09
IZn	513.27	0.25	442.28	−0.26	496.37	0.01	380.87	0.22
IMn	−365.38	−0.09	−524.50	0.65	−872.40	−0.56	−622.09	−0.28
Ife	865.11	0.77	773.28		921.22	0.61	897.74	0.64
IBN	432.86		428.73		550.18		505.45	
SD	490.50		476.06		633.27		565.73	

Legend: RAPNs—Response to Nutrient Application Potential, IBN—the nutritional balance index.

The nutritional balance index found in our samples showed a deficiency of natrium, potassium, calcium, magnesium, sulfur, and mangan in the case of all samples of healthy and symptomatic plants in all three stages of the bud rot. In stage II, leaves showed a higher value of deficiency in natrium (−517.24), calcium (−360.95), and mangan (−872.40), while leaves in stage III showed low levels of magnesium (−411.53) and sulfur (−430.52). The healthy plants showed a higher value of the indices of phosphorus (−622.36) (Table 4).

3.2. Metagenomic Analysis

MiSeq outcome for the ribosomal ITS1 region was analyzed for each sample, obtaining 13.591 reads for the infected soil sample (A), 20.733 reads for the healthy soil sample (B), 292.437 reads for the infected plants sample (C) and 257.989 reads for the healthy plants sample (D). Each group per sample consists of 100% of Reads Passing Quality Filtering (Figure 2).

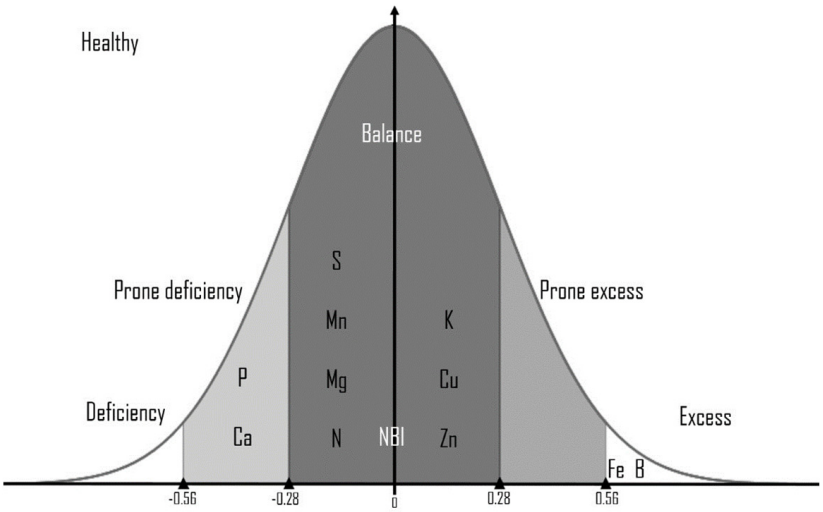

Figure 1. *Cont.*

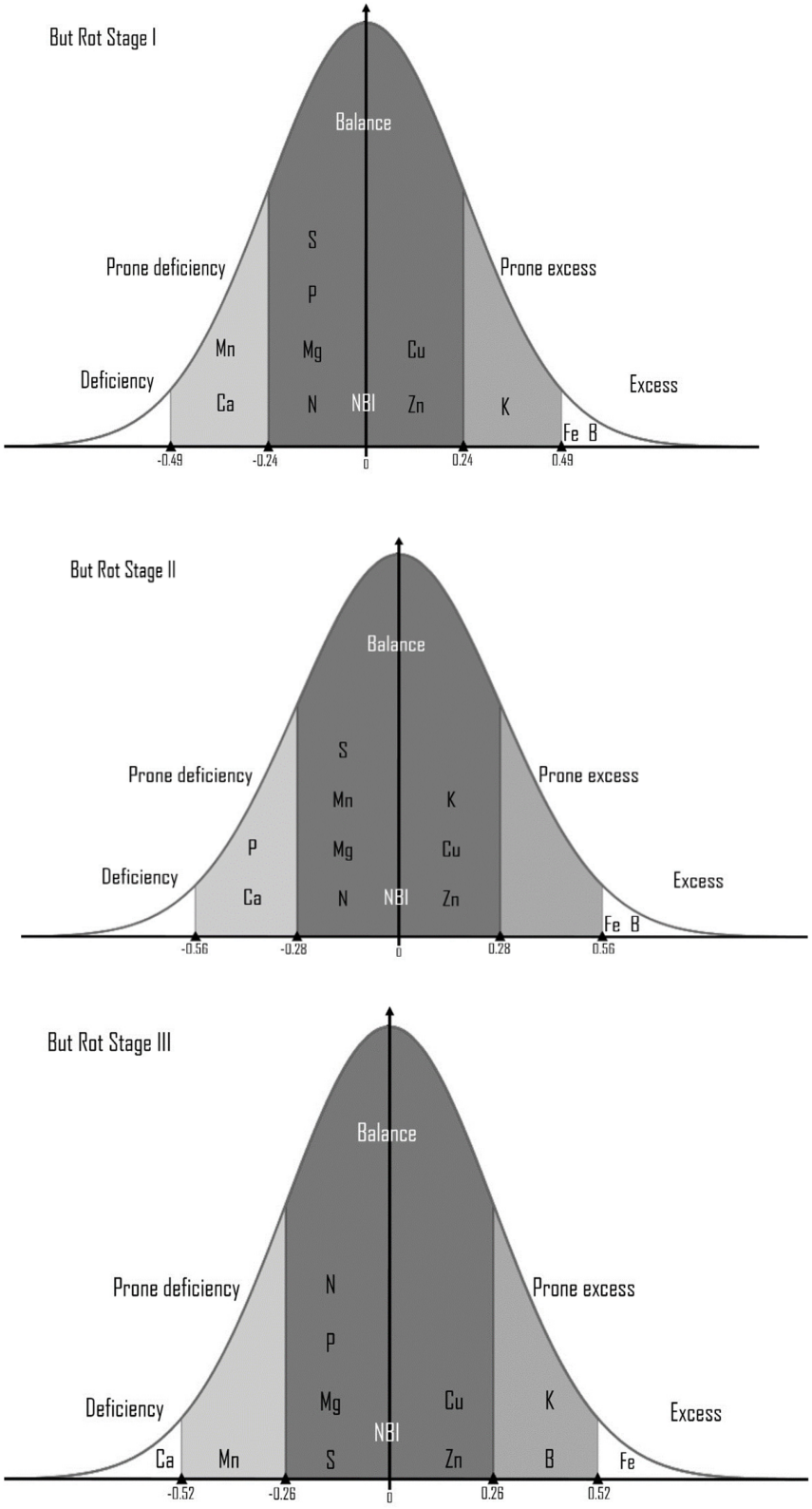

Figure 1. The soil nutrient variation on *E. guineensis* faces different bud rot disease stages.

In all samples, a different abundance of fungi sequences (95.1% in (A), 96.45% in (B), 99.68% in (C), and 99.58% in (D)) were registered. At the phylum level, the sequence abundance is presented in Figure 3.

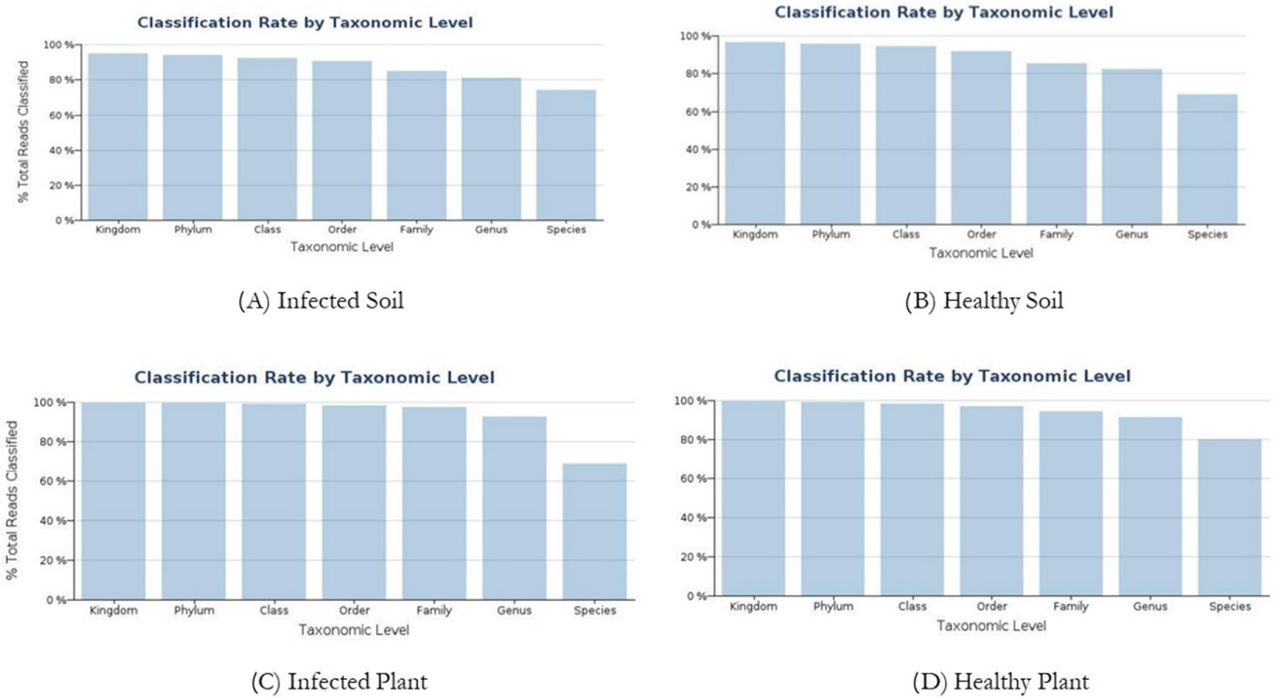

Figure 2. Histogram describes the number of species and sequences distributed per kingdom, phylum, class, order, family, genus, and species.

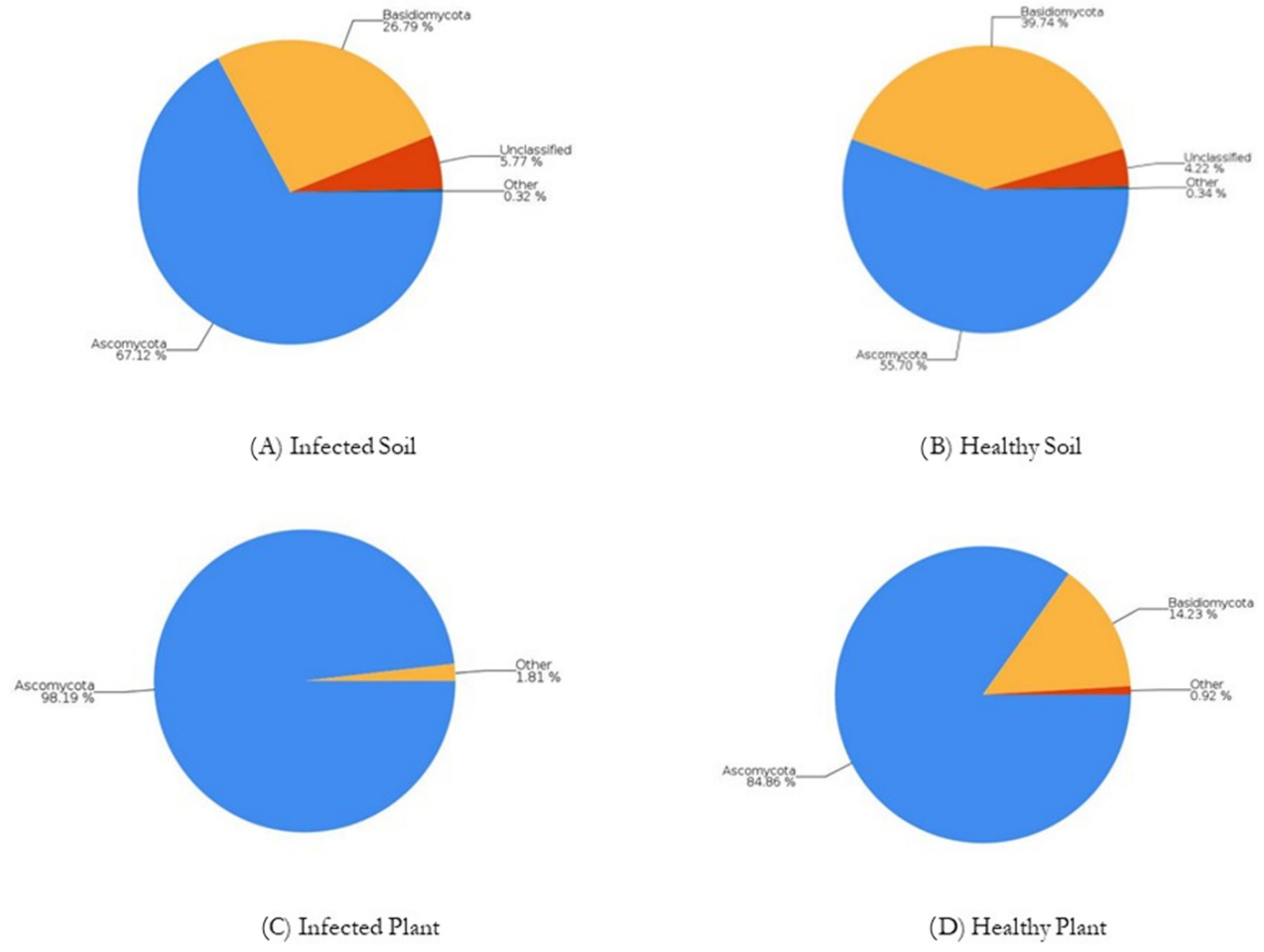

Figure 3. The abundance (%) of sequences and identified at the phylum level for samples.

The number of sequences that were analyzed in our trimmed dataset for each sample demonstrated that three major fungal genus pathogens were found in leaf and soil samples in plants that were healthy and at stage I of infection, which were defined as *Ascochyta*, *Colletotrichum*, and *Fusarium*, as seen in Table 5. The occurrence of the basidiomycete Antrodia is remarkable.

Table 5. The abundance (%) of sequences and identified at the species level for samples.

Category	Abundance %			
	A Infected Soil	B Healthy Soil	C Infected Plant	D Healthy Plant
Unclassified at the species level	25.8	30.89	31.03	19.78
Ascochyta rabiei (A)	20.79	9.3		
Talaromyces ruber (A)	9.76	7.71		
Cryptococcus neoformans (B)	6.58	5.5		
Antrodia sp. (B)	3.43	3.25		
Saccharomyces sp. (A)	3.37	7.9		
Candida sake (A)	3.06			
Pyrenochaetopsis leptospora (A)	1.98			
Wallemia sebi (B)		2.37		
Acanthocorticium brueggemannii (B)		1.99		
unidentified Hypocreales fam *Incertae sedis* sp.			22.91	5.47
Colletotrichum clidemiae (A)			17.41	
Plectosphaerella cucumerina (A)			12.93	2.33
Acremonium stromaticum (A)			5.49	
Fusarium solani (A)			2.1	11.54
Fusarium neocosmosporiellum (A)			1.99	1043
Plectosphaerella oratosquillae (A)			0.8	
Cryptococcus nanyangensis (B)				7.57
Xenoacremonium recifei (A)				4.21
Fusarium ramigenum (A)				3.88
Wallemiales (B)			0.74	
Myrmecridiales (A)			0.4	
Magnaporthales (A)			0.28	
Capnodiales (A)				2.53

Legend: A—Ascomycota, B—Basidiomycota.

Between samples represented by leaves from infected plants and soil collected around from infected plants, no common fungi were registered: only a different percentage of unclassified ones at the species level.

Comparing soil samples, it can be observed that a higher abundance of different fungi characterizes the soil collected around infected plants (A) with *Ascochyta rabiei* being identified as the major pathogenic fungi species present. The same tendency may be observed in the plant samples with the mention that *Fusarium solani and Fusarium neocosmosporiellum* have a higher abundance in healthy plants (D). Moreover, the pathogenic fungi *Colletotrichum clidemiae* had been identified in the infected plant samples, and *Plectosphaerella* spp. had been identified in both infected and healthy plants.

The unique orders found in samples were represented by *Wallemiales* (0.47%), *Myrmecridiales* (0.4%), and *Magnaporthales* (0.28%) in infected plants (C) and *Capnodiales* (2.53%) in healthy plants (D).

3.3. Liquid Chromatography-Mass Spectrometry (LC-MS) Analysis

The chromatograms were examined in full-scan mode, which revealed the presence of different compounds that were identified after the comparison with available standards, as listed in Table 6 and Figure 4. The compounds identified through the LC-MS method were represented by phenolic precursors (such as shikimic acid and caffeyl alcohol), flavonoids,

epicatechin, kaempferol-7-O-neohesperidoside, naringenin-7-O-glucoside, isovitexin, rutin and flavonoid glycosides.

Table 6. Total ion chromatogram (TIC) of the phenolic compounds identified in *E. guinensis* by LC-MS method in negative mode.

Identified Compound	Molecular Formula	Ion Adduct	Molecular Weight (g/mol)	LC-MS		
				[M-H]−	rt	Fr
Shikimic acid	$C_7H_{10}O_5$	M − H	174.15	173.045	1.191	
Epicatechin	$C_{15}H_{14}O_6$	M − H	290.07904	289.072	1.609	
(10E,15E)-9,12,13-trihydroxyoctadeca-10,15-dienoic acid	$C_{18}H_{32}O_5$	M − H	328.4	327.218	21.467	3
[(4E)-7-acetyloxy-6-hydroxy-2-methyl-10-oxo-2,3,6,7,8,9-hexahydrooxecin-3-yl] (E)-but-2-enoate	$C_{16}H_{22}O_7$	M + H	326.34	325.129	31.257	
[5-acetyloxy-3-(hydroxymethyl)-2-oxo-6-propan-2-ylcyclohex-3-en-1-yl] 3-methyl pentanoate	$C_{18}H_{28}O_6$	M + H	340.4	339.181	32.56	
1-[2-methyl-6-[(2S,3R,4S,5S,6R)-3,4,5-trihydroxy-6-(hydroxymethyl)oxan-2-yl]oxyphenyl]ethanone	$C_{14}H_{18}O_7$	M + H	298.29	311.114	32.046	21, 2, 12, 17, 5, 2
8-hydroxy-2,7,7,11,15-pentamethyl-5,12,16-trioxapentacyclo[9.8.0.0(2),.0,.0(1)(3),(1)]nonadec-13(18)-ene-3,17-dione	$C_{21}H_{28}O_6$	M − H	376.4	377.102	1.14	
alpha, alpha-Trehalose	$C_{12}H_{22}O_{11}$	M − H	342.297	387.115	1.14	15
Carnosine	$C_9H_{14}N_4O_3$	M + H	226.23	225.099	41.607	2, 3
Cystine	$C_6H_{12}N_2O_4S_2$	M + H	240.3	239.017	41.913	9, 1
DOCOSANOL	$C_{22}H_{46}O$	M + H	326.6	325.348	34.004	
Ethylenediaminetetraacetic acid	$C_{10}H_{16}N_2O_8$	M − H	292.24	291.084	31.676	3
IS_N-BENZOYL-D5-GLYCINE	$C_9H_9NO_3$	M − H	184.2	183.082	1.191	4
Canrenone	$C_{22}H_{28}O_3$	M − H	340.2038	339.197	28.852	7, 3
Isoorientin	$C_{21}H_{20}O_{11}$	M − H	448.38	447.093	13.429	3, 3
Massbank:IA000081 9-HODE	$C_{18}H_{32}O_3$	M − H1	296.235	295.228	32.232	7
Massbank:IA000367 9-HOTrE	$C_{18}H_{30}O_3$	M − H1	294.219	293.212	30.656	3
Citric acid	$C_6H_8O_7$	M + H	192.12	191.02	1.191	2
n-Capric acid	$C_{10}H_{20}O_2$	M − H	172.146	171	1.123	
Furosemide	$C_{12}H_{11}ClN_2O_5S$	M − H	330.0077	329	30.21	2
2-Hydroxyhippuric acid | 2-hydroxyhippurate	$C_9H_9NO_4$	M − H	195.05316	194.1	28.272	
Kaempferol-7-O-neohesperidoside	$C_{27}H_{30}O_{15}$	M − H	594.15847	593.151	1.566	2
Naringenin-7-O-glucoside	$C_{21}H_{22}O_{10}$	M − H	434.397	433.114	32.002	
Isovitexin	$C_{21}H_{20}O_{10}$	M − H	432.381	431.098	1.744	1
Caffeyl alcohol	$C_9H_{10}O_3$	M − H	166.176	165.056	1.158	
Massbank:PR309095 FA 18:2 + 2O	$C_{18}H_{32}O_4$	M − H	312.45	311.222	29.94	
Massbank:PR309165 MGMG 18:3	$C_{27}H_{46}O_9$	M + HCOO	514.656	559.312	31.229	3
Massbank:PR309165 MGMG 18:3	$C_{27}H_{46}O_9$	M + HCOO	514.656	559.312	31.658	1
Massbank:PR309171 DGMG 18:3	$C_{33}H_{56}O_{14}$	M + HCOO	676.8	721.363	29.236	3, 6
Coumaroyl + C6H9O8 (isomer of 844, 845, 846)	$C_{15}H_{16}O_{10}$	M − H	356.28	355.065	1.557	8
Massbank:UT000256 9-HPODE	$C_{18}H_{32}O_4$	M − H	312.23006	311.223	29.191	5
Massbank:UT000264 9-HpOTrE	$C_{18}H_{30}O_4$	M − H	310.21441	309.207	28.062	1
Dodecylbenzenesulfonic acid	$C_{18}H_{30}O_3S$	M-H	326.19157	325.184	29.94	8
Rutin	$C_{27}H_{30}O_{16}$	M − H	610.15338	609.146	1.557	
Sesamin	$C_{20}H_{18}O_6$	M + H	354.4	353.103	33.906	14
Sucrose	$C_{12}H_{22}O_{11}$	M − H	342.3	341.109	1.14	
Thymol-beta-D-glucoside	$C_{16}H_{24}O_6$	M + H	312.36	311.15	34.672	
Trihydroxy flavone-C-hexoside-C-pentoside	$C_{27}H_{30}O_{15}$	M − H	594.5	563.141	1.557	2

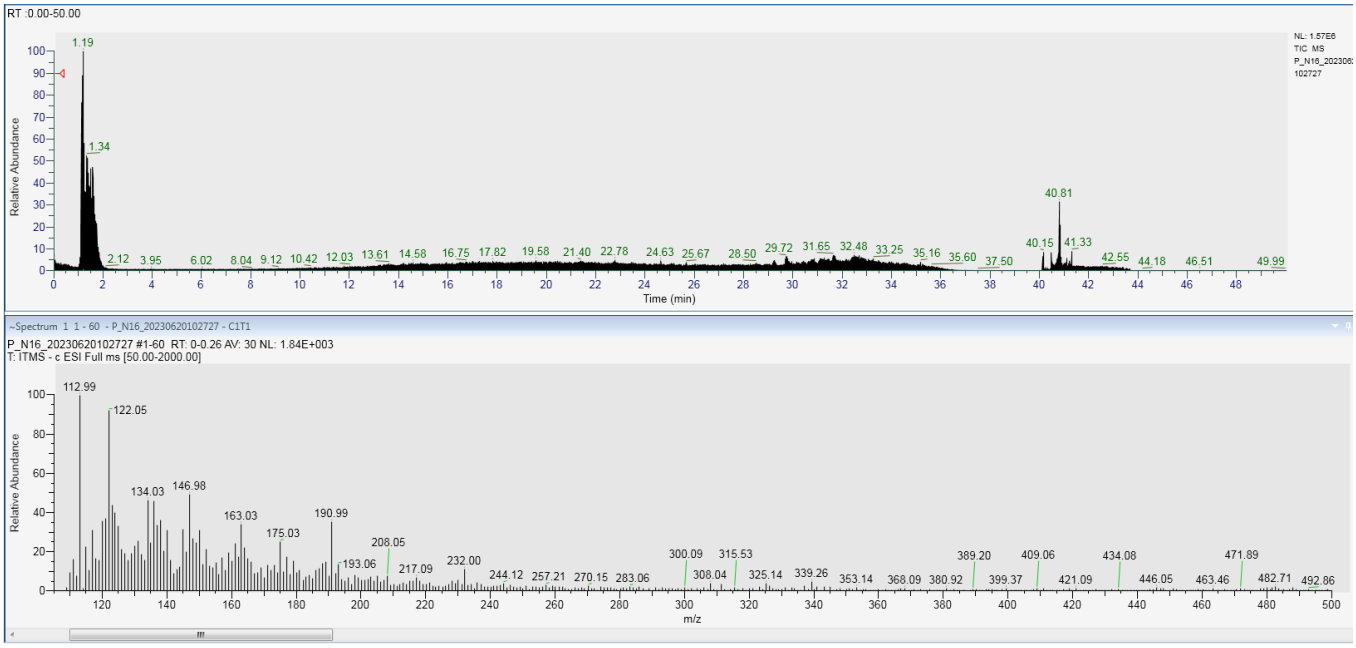

Figure 4. LC-MS chromatograms of compounds from *E. guinensis* samples.

4. Discussion

4.1. The Diagnosis and Recommendation Integrated System—DRIS

The estimation of the nutrients provides information concerning the different environmental pressures [47]. DRIS represents a technique applied in plant analysis (nutrient concentration) to diagnose the most limiting nutrient, exhibiting a weaker effect of environmental factors [48]. The DRIS methodology consists of the transformation of nutrients into indices (standardized by Gaussian distribution) and expressed reported to the degree of limitation from the greatest deficiency to highest excess. The nutrient index is expressed as positive and negative values. Positive indexes showed that the nutrients were in "excess" and negative indexes indicated that the nutrients were "deficient" in plants.

Our DRIS analysis underlined a light deficiency of Ca^{2+} ions in healthy oil palms that increases during the infection stages of bud rot disease. It is known that calcium is an essential element in plants that serves as a constituent of cell walls and membranes, contributing to the structure of cells and upholding physical barriers against pathogens. By its structural role, plants deficient in calcium are more susceptible to pathogens, and exogenous calcium supply, in turn, has been shown to improve the plant's resistance; calcium serves as a second messenger being interconnected with the signaling of other nutrients as well as pathogen attack [49]. So, the Ca deficiency registered in oil palm can be the main reason for the susceptibility of this crop to any pathogen attack and in our case could be the initial indication of bud rot in this crop. Mn is another deficient nutrient identified by DRIS analysis in oil palm, which is an important co-factor of different enzyme fundamentals for the biosynthesis of secondary metabolites associated with the shikimic acid pathway including phenolics, coumarins, lignin, and flavonoids [50]. Also, this deficiency can be one of the principal causes of the palm debility and susceptibility front of diseases. DRIS analysis revealed an excessive concentration of Fe in oil palm in all the disease stages and even in healthy palms. Iron is an essential nutrient for plants, playing an important role in the electron-transport chains of photosynthesis and respiration. At high levels, iron is toxic due to its capacity to act catalytically via the Fenton reaction to generate hydroxyl radicals, which can damage lipids, proteins, and DNA [51] and in conclusion can produce stress on oil palm levels that can make it more susceptible to pathogen damages. In the second stage of bud rot disease, oil palm presents a deficiency of Mg and Mn nutrients, not only Ca.

Our results are based on those of Viégas et al., 2000 [52], which underline the influence of iron in the disease.

4.2. Metagenomic Analysis

Palm plantations have been affected by several diseases. The ones that stand out most among them are bud rot, root and trunk rot, lint disease, red ring, and others [53]. But rot is a disease with various effects from lower ones to the destruction of crops. There is a scale (CENIPALMA) for bud rot symptomatology: the healthy stage (with no lesions of the emerging leaf), stage 1 (lesions account for between 0.1% and 20% of the emerging leaf), stage 2 (the lesions cover between 40.1% and 60% of the emerging leaf) and stage 3 (lesions are spread between the 80.1% and 100% of the emerging leaf) [54].

Fungi, being decomposers, pathogens, and plant mutualists, have important roles in the ecosystem. These organisms are the most dominant groups in soil [55].

Although *Phytophthora palmivora* Butl has already been described as the causative agent for the first lesions, opportunistic pathogens might appear [56]: various fungi (*Fusarium* spp., *Colletotrichum* sp., *Thielaviopsis* sp., and *Rhizoctonia* sp., among others), bacteria (*Pseudomonas* sp. and *Erwinia* sp.) and insects (*Rhynchophorus palmarum*) that promote the rotting process. These biological agents have a high incidence in the death rate of the oil palm.

Previous studies carried out in Surinam [55] treating bud rot disease have isolated *Fusarium* spp., *Botrydiplodia* spp., *Colletotrichum* spp., and the *Erwinia amylovora* bacterium, while in Ecuador, a study regarding fungal diseases in oil palms identified *Fusarium* spp. followed by *Colletotrichum* spp., *Lasiodiplodia* spp., *Pestalotia* spp., *Nigrospora* spp., *Curvularia* spp. and *Trichoderma* spp. [57]. In the present study, an abundance of 17.41% of *Colletotrichum* spp. was found in the leaves of infected plants, while *F. solani* presented an abundance of 2.1% in infected plants and 11.54% in healthy plants in addition to the presence of *F. neocosmosporiellum* both in infected (1.99%) and healthy (10.43%) plants.

Fungal diversity in oil palms plays a key role in the development of rot diseases, as described in the identification of several fungal pathogens, whilst in addition to the most abundant groups, *Colletotrichum* spp., an important plant pathogen, appears as the predominant group in diseased samples [58]. As the literature dictates, pathogens of the genus *Colletotrichum* are responsible for anthracnose diseases in various economically important crops [59], such as oil palms. Anthracnose, caused by *Colletotrichum* spp., is an important disease that affects palm trees especially since the fungus can survive in the debris of the previous year's infected bunches for up to 8 months [60].

Ascomycota and *Basidiomicota* are the most common phylum found in all our samples. Our data are based on Wong et al., 2021 [61], which found that *Ascomycota* and *Basidiomicota* are the most frequent phylum found in the oil palm planted areas. *Ascomycota* was reported to be the dominant fungal group in plant tissues and different soil types and fertilizers [22]. It is predominantly terrestrial, generally, saprophytes on decaying plant debris contribute to the nutrient cycling in the ecosystems [62]. Also, *Basidiomycota* are important decomposers.

Harvested oil palm trunks with their high moisture content are very susceptible to rot by wood decay via Basidiomycota. The brown rot fungus *Coniophora puteana* and the white rot species *Pleurotus ostreatus* decayed oil palm trunk samples with mass loss of up to 50% within 1 month of incubation [63].

Different steps of plant growth and development (like metabolism, nutrient regulation, reproduction, chlorophyll synthesis, carbohydrate production, fruit, and seed development, etc.) are performed by an adequate level of micro and macronutrients. The presence of decomposers is affecting the nutrients present in soils. A deficiency or excess of nutrients negatively influence the plant's physiological, biochemical, and metabolic characteristics and can promote even abnormal growth and susceptibility in front of pathogens [64].

4.3. LC-MS Analysis

Recently, many bioactive compounds have been isolated that have contributed to the understanding of their role in the immune system of plants. Many natural compounds act as inducers of defense responses in plants [65]. The indirect action of bioactive compounds on plant cells stimulates the release of protein and lipid elicitors [66], leading to the synthesis of phytoalexins and pathogenesis-related proteins, the accumulation of callose and lignification of the cell wall, as well as increased activity of several defense enzymes, which protects plants against pathogens [67].

In the present study, different flavonoid compounds were identified through the LC-MS method. Flavonoids play an important role in the defense mechanism of the plant. In addition to acting as UV filters, signal molecules, allopathic chemicals, phytoalexins, detoxifying agents, and antimicrobials, flavonoids protect plants against biotic and abiotic stress [68]. The anti-pathogenic properties of flavonoids may result from their antioxidant properties influencing the deactivation of ROS generated by both pathogens and the plant as a result of infection [69].

Epicatechin is a known flavonoid with biological activity mainly attributed to its interaction with proteins and lipids and its antimicrobial properties essential for resistance in plant diseases [66], since it has been reported to inhibit appressorial melanization of the necrotrophic fungus *Colletotrichum kahawae* that causes coffee berry disease [70].

Rutin has also been identified in the plant sample, which is one of the huge families of flavonoids that was widely distributed in Plantae [71]. Like other flavonoids, rutin acts to reduce environmental stress, e.g., via UV-B screening, antioxidant activity, and disease resistance, through an increase in quercetin and rutinose concentrations [72].

Kaempherol and its glycosides, such as kaempferol 7-neohesperidoside identified in stage I of infection, have antibacterial, antiviral, antifungal, and antiprotozoal activities, as it has been reported in numerous papers [73–75]. Naringenin is a flavonoid classified as a flavanone, and it is widely distributed in several fruits and found in its glycoside form as well [76]. Recently, An et al., 2021 [77] found that naringenin induces pathogen resistance, suggesting that pathogen-accumulated naringenin leads to pathogen resistance, which is related to its known biological functions like other flavonoids.

Flavones, a subclassification of flavonoids, had also been identified in the present study, such as isoorientin and isovitexin, which are described as C-glycosyl flavonoids and are found in different plants [78]. Flavones have a variety of functions for the plant defense mechanism, similar to flavonoids, including interactions between species like resistance to pathogens, symbiosis, protection against herbivory, and allelopathy [79,80].

5. Conclusions

The present study has focused on the biotic and abiotic factors represented by nutrient deficiency or excess, which trigger an increased susceptibility of the oil palm to any pathogenic attack and can cause a high disease incidence. The involvement of elements such as Ca, Fe, Mn, and Mg in the palm debility front of pathogens causing bud rot disease was proved. In the case of biotic factors, our study indicates that cumulative fungi are implied in bud rot disease. A very important role was played by the combination of biotic and abiotic factors. Numerous compounds (with protective roles) were identified in the leaves of symptomatic plants from stage I of the infection. The early identification of the determining factors of the disease (lack of minerals or pathogens present in the soil and/or plant) may contribute to the reduction in the disease incidence by isolating the affected specimens.

Author Contributions: Conceptualization, R.A.M.; methodology, R.A.M. and E.J.M.H.; software, R.A.M. and E.J.M.H.; validation, R.A.M.; formal analysis, P.A.L.A., R.A.M. and E.J.M.H.; investigation, R.A.M. and E.J.M.H.; writing—original draft preparation, R.A.M., E.J.M.H. and R.D.C.; writing—review and editing, R.A.M. and R.D.C.; project administration, R.A.M.; funding acquisition, R.A.M. All authors have read and agreed to the published version of the manuscript.

Funding: This research was funded by Universidad de las Fuerzas Armadas—ESPE, grant number CV-GNP-0012-2017, and Romanian Academy, grant number RO1567-IBB08/2023.

Institutional Review Board Statement: Not applicable.

Informed Consent Statement: Not applicable.

Data Availability Statement: Not applicable.

Acknowledgments: Our scientific team gratefully acknowledges the material and financial support of The Unit of Management of Linkage with Society from Universidad de Las Fuerzas Armadas-ESPE, which helped us undertake this study. Additionally, we would like to give thanks to INIAP Santo Domingo, especially to Digner Ortega for offering us support and technical advice for the collection material. In particular, we are thankful for the sincere and constant support, availability, professionalism, and kindness of the agricultural engineer Richard Carrera and Rafael Silva Mancheno. We are grateful to the poet Carrie J. Myers, who had the amiability to revise the English.

Conflicts of Interest: The authors declare no conflict of interest. The funders had no role in the design of the study; in the collection, analyses, or interpretation of data; in the writing of the manuscript; or in the decision to publish the results.

References

1. Rozali, N.; Yarmo, M.; Abu Seman, I.; Kushairi, A.; Ramli, U. Metabolomics differentiation of oil palm (*Elaeis guineensis* Jacq.) spear leaf with contrasting susceptibility to *Ganoderma boninense*. *Plant Omics J.* **2017**, *10*, 45–52. [CrossRef]
2. Naher, L.; Yusuf, U.K.; Ismail, A.; Tan, S.G.; Mondal, M.M.A. Ecological status of *Ganoderma* and basal stem rot disease of oil palms (*Elaeis guineensis* Jacq.). *Aust. J. Crop Sci.* **2013**, *7*, 1723–1727.
3. Owoyele, B.V.; Owolabi, G.O. Traditional oil palm (*Elaeis guineensis* Jacq.) and its medicinal uses: A review. *Cell Med.* **2014**, *4*, e16. [CrossRef]
4. Nair, P.K. Tree Crops. In *Harvesting Cash from the World's Important Cash Crops*, 1st ed.; Springer Nature: Cham, Switzerland, 2021; pp. 249–285.
5. Widiastuti, H.; Taniwiryono, D.; Hendarjanti, H.; Harjotedjo, S. Chemical and biological characteristics of selected wet soil in oil palm plantation attack with *Ganoderma* sp. *IOP Conf. Ser.* **2018**, *183*, 012019. [CrossRef]
6. Chung, G.F. Effect of pests and diseases on oil palm yield. In *Palm Oil*; AOCS Press: Urbana, IL, USA, 2012; pp. 163–210.
7. Aderungboye, F.O. Diseases of the oil palm. *Int. J. Pest Manag.* **1977**, *23*, 305–326. [CrossRef]
8. Viera-Torres, M.; Sinde-González, I.; Gil-Docampo, M.; Bravo-Yandún, V.; Toulkeridis, T. Generating the Baseline in the Early Detection of Bud Rot and Red Ring Disease in Oil Palms by Geospatial Technologies. *Remote Sens.* **2020**, *12*, 3229. [CrossRef]
9. Benítez, É.; García, C. The history of research on oil palm bud rot (*Elaeis guineensis* Jacq.) in Colombia. *Agron. Colomb.* **2014**, *32*, 390–398. [CrossRef]
10. Sarria, G.A.; Torres, G.A.; Aya, H.A.; Ariza, J.G.; Rodríguez, J.; Vélez, D.C.; Varón, F.; Martínez, G. *Phytophthora* sp. es el responsable de las lesiones iniciales de la pudrición de cogollo (PC) de la palma de aceite en Colombia. *Palmas* **2008**, *29*, 31–41.
11. Franqueville, H. Oil palm Bud Rot in latín America. *Exp. Agric.* **2003**, *39*, 225–240. [CrossRef]
12. Available online: https://oec.world/en/profile/bilateral-product/palm-oil/reporter/ecu?redirect=true (accessed on 15 January 2023).
13. Instituto Nacional de Estadística y Censos [INEC]. *Manual del Encuestador y Supervisor "Encuesta de Superficie y Producción Agropecuaria Continua ESPAC" 2019*; Instituto Nacional de Estadistica y Censos: Quito, Ecuador, 2019.
14. Allen, W.; Paulus, A.; van Gundy, S.; Swinburne, T.R.; Ollagnier, M.; Renard, J.L. Report on the mission to Ecuador. In *Document Cirad-Cp*; Palmeras del Ecuador-Palmoriente: Montpellier, France, 1995.
15. Gómez, P.; Ayala, L.; Munévar, F. Characteristics and management of bud rot, a disease of oil palm. In *Plantation Tree Crops in the New Millennium: The Way Ahead*; Pushparajah, E., Ed.; The Incorporated Society of Planters: Kuala Lumpur, Malaysia, 2000; Volume 1, pp. 545–553.
16. Albertazzi, H.; Bulgarelli, J.; Chinchilla, C. Onset of spear root symptoms in oil palm and prior (and contemporary) events. *ASD Oil Palm Pap.* **2005**, *21*, e41.
17. Gunasinghe, N.; Mingpei, P.Y.; Cawthray, G.R.; Barbetti, M.J. Cercosporin from *Pseudocercosporella capsellae* and its critical role in white leaf spot deveelopment. *Plant Dis.* **2016**, *100*, 1521–1531. [CrossRef] [PubMed]
18. Avendaño, J.C.; Garzon, G.M. Experiencias del manejo de la pudrición del cogollo (PC) en *Elaeis guineensis* y el híbrido OxG en Astorga S.A. *Palmas* **2013**, *34*, 77–88.
19. Aya, H.; Varón, F.; Martínez, G.; Cayón, G. Manejo químico de la Pudrición de cogollo en cuatro materiales de palma de aceite en Tumaco. *Rev. Palmas-Colomb.* **2011**, *32*, 45–52.
20. Torres, G.A.; Sarria, G.A.; Martínez, G. *Identificación Temprana y Manejo de la Pudrición del Cogollo de la Palma de Aceite*, 1st ed.; Cenipalma-Fedepalma-Sena SAC: Bogotá, Colombia, 2010.

21. Bennett, A.J.; Bending, G.D.; Chandler, D.; Hilton, S.; Mills, P. Meeting the demand for crop production: The challenge of yield decline in crops grown in short rotations. *Biol. Rev.* **2012**, *87*, 52–71. [CrossRef] [PubMed]
22. Kirkman, E.R.; Hilton, S.; Sethuraman, G.; Elias, D.M.O.; Taylor, A.; Clarkson, J.; Soh, A.C.; Bass, D.; Ooi, G.T.; McNamara, N.P.; et al. Diversity and Ecological Guild Analysis of the Oil Palm Fungal Microbiome Across Root, Rhizosphere, and Soil Compartments. *Front. Microbiol.* **2022**, *13*, 792928. [CrossRef] [PubMed]
23. Kazeeroni, E.A.; Al-Sadi, A.M. 454-pyrosequencing reveals variable fungal diversity across farming systems. *Front. Plant Sci.* **2016**, *7*, 314. [CrossRef] [PubMed]
24. Pagare, S.; Manila, B.; Niraj, T.; Pagare, S.; Bansal, Y.K. Secondary Metabolites of Plants and their Role: Overview. *Curr. Trends Biotechnol. Pharm.* **2015**, *9*, 293–304.
25. Ramírez-Orellana, A.; Ruiz-Palomo, D.; Rojo-Ramírez, A.; Burgos-Burgos, J.E. The Ecuadorian Banana Farms Managers' Perceptions: Innovation as a Driver of Environmental Sustainability Practices. *Agriculture* **2021**, *11*, 213. [CrossRef]
26. Ricaurte, D.V. *Inventario y Georeferenciación de los Principales Riesgos en la Ciudad de Quinindé—Provincia de Esmeraldas*; IAEN: Esmeraldas, Ecuador, 2011; p. 73.
27. Direction de Planification GADPE Prefectura Esmeraldas—Plan de Desarrollo Y Ordenamiento Territorial 2015–2025. Available online: https://www.prefecturadeesmeraldas.gob.ec/web/assets/2017{-}{-}pdot-gadpe-septiembre.pdf (accessed on 23 February 2023).
28. Gobierno Autónomo Descentralizado de la Provincia de Esmeraldas [GADPE]. 2012. Available online: https://prefecturadeesmeraldas.gob.ec/ (accessed on 23 February 2023).
29. Marrocos, P.C.L.; Loureiro, G.A.H.D.A.; De Araujo, Q.R.; Sodré, G.A.; Ahnert, D.; Baligar, V.C. Mineral nutrient ratios and cacao productivity. *J. Plant Nutr.* **2020**, *43*, 2368–2382. [CrossRef]
30. Gieseking, J.E.; Snider, H.J.; Getz, C.A. Destruction of organic matter in plant material by the use of nitric and perchloric acids. *Ind. Eng. Chem. Anal.* **1935**, *7*, 185–186. [CrossRef]
31. Gee, A.; Domingues, L.; Dietz, V. Constituents in sugar. *Anal. Chem.* **1954**, *26*, 1487–1492. [CrossRef]
32. Matos, G.S.B.; Fernandes, A.R.; Wadt, P.G.S.; Pina, A.J.A.; Franzini, V.I.; Ramos, H.M.N. The use of DRIS for nutritional diagnosis in oil palm in the state of Pará. *Rev. Bras. Cien. Solo* **2017**, *41*, e0150466. [CrossRef]
33. de la Torre, A.; Iglesias, I.; Carballo, M.; Ramírez, P.; Muñoz, M.J. An approach for mapping the vulnerability of European Union soils to antibiotic contamination. *Sci. Total Environ.* **2012**, *414*, 672–679. [CrossRef] [PubMed]
34. Beaufils, E.R. Diagnosis and recommendation integrated system (DRIS). *Soil Sci. Bull. Univ. Natal.* **1973**, *1*, 1–132.
35. Badotti, F.; De Oliveira, F.S.; Garcia, C.F.; Vaz, A.B.M.; Fonseca, P.L.C.; Nahum, L.A.; Oliveira, G.; Góes-Neto, A. Effectiveness of ITS and sub-regions as DNA barcode markers for the identification of *Basidiomycota* (Fungi). *BMC Microbiol.* **2017**, *17*, 42. [CrossRef] [PubMed]
36. Siddique, A.B.; Albrectsen, B.R.; Ilbi, H.; Siddique, A.B. Optimization of Protocol for Construction of Fungal ITS Amplicon Library for High-Throughput Illumina Sequencing to Study the Mycobiome of Aspen Leaves. *Appl. Sci.* **2022**, *12*, 1136. [CrossRef]
37. Al-Bulushi, I.M.; Bani-Uraba, M.S.; Guizani, N.S.; Al-Khusaibi, M.K.; Al-Sadi, A.M. Illumina MiSeq sequencing analysis of fungal diversity in stored dates. *BMC Microbiol.* **2017**, *17*, 72. [CrossRef]
38. Hoggard, M.; Vesty, A.; Wong, G.; Montgomery, J.M.; Fourie, C.; Douglas, R.G.; Biswas, K.; Taylor, M.W. Characterizing the Human Mycobiota: A Comparison of Small Subunit rRNA, ITS1, ITS2, and Large Subunit rRNA Genomic Targets. *Front. Microbiol.* **2018**, *9*, 2208. [CrossRef]
39. Al-Sadi, A.M.; Kazerooni, E.A. Illumina-MiSeq analysis of fungi in acid lime roots reveals dominance of Fusarium and variation in fungal taxa. *Sci. Rep.* **2018**, *8*, 17388. [CrossRef]
40. Bolger, A.; Lohse, M.; Usadel, B. Trimmomatic: A flexible read trimming tool for Illumina Sequence. *Bioinformatics* **2014**, *30*, 2114–2120. Available online: http://www.usadellab.org/cms/?page=trimmomatic (accessed on 23 February 2023). [CrossRef]
41. Fan, S.; Miao, L.; Li, H.; Lin, A.; Song, F.; Zhang, P. Illumina-based analysis yields new insights into the diversity and composition of endophytic fungi in cultivated *Huperzia serrata*. *PLoS ONE* **2020**, *15*, e0242258. [CrossRef] [PubMed]
42. Available online: https://unite.ut.ee/ (accessed on 15 February 2023).
43. Hashizume, H.; Taga, S.; Sakata, M.K.; Taha, M.H.M.; Siddig, E.E.; Minamoto, T.; Fahal, A.H.; Kaneko, S. Detection of multiple mycetoma pathogens using fungal metabarcoding analysis of soil DNA in an endemic area of Sudan. *PLoS Negl. Trop. Dis.* **2022**, *16*, e0010274. [CrossRef]
44. Irakli, M.; Skendi, A.; Bouloumpasi, E.; Chatzopoulou, P.; Biliaderis, C.G. LC-MS Identification and Quantification of Phenolic Compounds in Solid Residues from the Essential Oil Industry. *Antioxidants* **2021**, *10*, 2016. [CrossRef] [PubMed]
45. Kang, J.; Price, W.E.; Ashton, J.; Tapsell, L.C.; Johnson, S. Identification and characterization of phenolic compounds in hydromethanolic extracts of. *Food Chem.* **2016**, *211*, 215–226. [CrossRef] [PubMed]
46. Bikoro Bi Athomo, A.; Engozogho Anris, S.P.; Safou Tchiama, R.; Eyma, F.; Arnaudguilhem, C.; Charrier, B. Identification of phenolic compounds from *K. Ivorensis* by selected chromatographic and spectrometric techniques. *J. Renew. Mat.* **2021**, *9*, 35–48. [CrossRef]
47. OECD. Nutrient Balance (Indicator). 2023. Available online: https://doi.org/10.1787/82add6a9-en (accessed on 8 June 2023).
48. Wadt, P.G.S.; Dias, J.R.M. Premises for DRIS application in forest species and palms. In *Nutrition and Fertilization of Forest Species and Palms*; Prado, R.M., Wadt, R.M.P.G.S., Eds.; FUNEP: Jaboticabal, Brazil, 2014; pp. 277–298.
49. Thor, K. Calcium—Nutrient and Messenger. *Front. Plant Sci.* **2019**, *10*, 440. [CrossRef] [PubMed]

50. Santos-Sánchez, N.F.; Salas-Coronado, R.; Hernández-Carlos, B.; Villanueva-Cañongo, C. Shikimic Acid Pathway in Biosynthesis of Phenolic Compounds. In *Plant Physiological Aspects of Phenolic Compounds*; IntechOpen: London, UK, 2019.
51. Connolly, E.L.; Guerinot, M.L. Iron stress in plants. *Genome Biol.* **2002**, *3*, 1–4. [CrossRef]
52. Viégas, I.J.M.; Furlan, J.J.; Frazão, D.A.C.; Batista, M.M.F. Influência do micronutriente ferro naocorrência do amarelecimento fatal do dendezeiro. *Tech. Bull.* **2000**, 32–37.
53. Abad, V. *Análisis Etiológico de la Enfermedad Pudrición del Cogollo (PC) en Cultivo de Palma Aceitera (Elaeis guineensis Jacq.) en la Provincia de Esmeraldas, Ecuador*; Universidad de Barcelona: Barcelona, Spain, 2022; Available online: https://www.tdx.cat/bitstream/handle/10803/675558/VMAV_TESIS.pdf?sequence=1&isAllowed=y (accessed on 13 April 2023).
54. Orgiazzi, A.; Lumini, E.; Nilsson, R.H.; Girlanda, M.; Vizzini, A. Unravelling soil fungal communities from different Mediterranean land-use backgrounds. *PLoS ONE* **2012**, *7*, e34847. [CrossRef]
55. Ramírez, M.; Benítez, E. Pudrición del Cogollo, la terrible enfermedad que ataca la palma de aceite. *Crop Life Latinoamérica* 2013. Available online: https://www.croplifela.org/es/plagas/listado-de-plagas/pudricion-del-cogollo (accessed on 13 April 2023).
56. Sánchez-Potes, A. Enfermedades de la palma de aceite en América Latina. *Rev. Palmas* **1990**, *11*, 990.
57. Terrero, P.; Peñaherrera, S.; Vera, D.; Navarrete, B.; Herrera, M. Prospección De Enfermedades Fúngicas En Plantaciones De Palma Aceitera En La Provincia De Los Ríos. *Ecuad. Es Calid.* **2017**, *4*, 21–25. [CrossRef]
58. de Assis Costa, O.Y.; Tupinambá, D.D.; Bergmann, J.C.; Barreto, C.C.; Quirino, B.F. Correction: Fungal diversity in oil palm leaves showing symptoms of Fatal Yellowing disease. *PLoS ONE* **2021**, *16*, e0254042. [CrossRef] [PubMed]
59. Castillo, S.R.M.; Miller, S.; Stewart, J. *Colletotrichum* spp. and other fungi associated with anthracnose on *Coffea arabica* L. in Mérida State, Venezuela. *Summa Phytopathol.* **2022**, *48*, 99–111. [CrossRef]
60. Cao, X.; Xu, X.; Che, H.; West, J.S.; Luo, D. Eight *Colletotrichum* species, including a novel species, are associated with areca palm anthracnose in Hainan, China. *Plant Dis.* **2020**, *104*, 1369–1377. [CrossRef] [PubMed]
61. Wong, S.; Muharam, F.M.; Rashed, O.; Khairulmazmi, A. Soil fungal composition and diversity in oil palm plantation at Sungai ASAP, Sarawak, Malaysia. *J. Oil Palm Res.* **2021**, *33*, 215–226. [CrossRef]
62. Moore-Landecker, E. *Fundamentals of the Fungi*; Prentice-Hall, Inc.: Englewood Cliffs, NJ, USA, 1972; pp. 80–100.
63. Schmidt, O.; Bahmani, M.; Koch, G.; Potsch, T.; Brandt, K. Study of the fungal decay of oil palm wood using TEM and UV techniques. *Int. Biodeterior. Biodegrad.* **2016**, *111*, 37–44. [CrossRef]
64. Rahman, R.; Ahmad Sofi, J.; Javeed, I.; Hussain Malik, T.; Nisar, S. Role of Micronutrients in Crop Production. *Int. J. Curr. Microbiol. App Sci.* **2020**, *11*, 2265–2287.
65. Reglinski, T.; Walters, D. Induced Resistance for Plant Disease Control. In *Disease Control in Crops: Biological and Environmentally-Friendly Approaches*; John Wiley & Sons: Hoboken, NJ, USA, 2009. [CrossRef]
66. Koziara, W.; Sulewska, H.; Panasiewicz, K. Effect of resistance stimulator application to some agricultural crops. *J. Res. Appl. Agric. Eng.* **2006**, *51*, 82–86.
67. Jamiołkowska, A. Natural compounds as elicitors of plant resistance against diseases and new biocontrol strategies. *Agronomy* **2020**, *10*, 173. [CrossRef]
68. Mierziak, J.; Kostyn, K.; Kulma, A. Flavonoids as important molecules of plant interactions with the environment. *Molecules* **2014**, *19*, 16240–16265. [CrossRef]
69. Nabil-Adam, A.; Elnosary, M.E.; Ashour, M.L.; El-Moneam, N.M.A.; Shreadah, M.A. Flavonoids Biosynthesis in Plants as a Defense Mechanism: Role and Function Concerning Pharmacodynamics and Pharmacokinetic Properties. In *Flavonoid Metabolism—Recent Advances and Applications in Crop Breeding)*; Abbas, H.M.K., Ahmad, A., Eds.; IntechOpen: London, UK, 2023; p. 3. [CrossRef]
70. Zhang, R.; Wang, J.; Xia, R.; Li, D.; Wang, F. Antioxidant processes involving epicatechin decreased symptoms of pine wilt disease. *Front. Plant Sci.* **2022**, *13*, 1015970. Available online: https://www.frontiersin.org/articles/10.3389/fpls.2022.1015970 (accessed on 13 April 2023). [CrossRef] [PubMed]
71. Chen, Z.; Liang, J.; Zhang, C.; Rodrigues, C.J. Epicatechin and catechin may prevent coffee berry disease by inhibition of appressorial melanization of *Colletotrichum kahawae*. *Biotechnol. Lett.* **2006**, *28*, 1637–1640. [CrossRef] [PubMed]
72. Yang, W.; Xu, X.; Li, Y.; Wang, Y.; Li, M.; Wang, Y.; Ding, X.; Chu, Z. Rutin-Mediated Priming of Plant Resistance to Three Bacterial Pathogens Initiating the Early SA Signal Pathway. *PLoS ONE* **2016**, *11*, e0146910. [CrossRef] [PubMed]
73. Suzuki, T.; Morishita, T.; Kim, S.-J.; Park, S.-U.; Woo, S.; Noda, T.; Takigawa, S. Physiological Roles of Rutin in the Buckwheat Plant. *Jpn. Agric. Res. Q.* **2015**, *49*, 37–43. [CrossRef]
74. Chen, W.; Xiao, Z.; Wang, Y.; Wang, J.; Zhai, R.; Lin-Wang, K.; Espley, R.; Ma, F.; Li, P. Competition between anthocyanin and kaempferol glycosides biosynthesis affects pollen tube growth and seed set of *Malus*. *Hort. Res.* **2021**, *8*, 173. [CrossRef] [PubMed]
75. Cid-Ortega, S.; Monroy-Rivera, J.A. Extraction of Kaempferol and Its Glycosides Using Supercritical Fluids from Plant Sources: A Review. *Food Tech. Biotechnol.* **2018**, *56*, 480–493. [CrossRef] [PubMed]
76. De Melo, G.O.; Malvar, D.d.C.; Vanderlinde, F.A.; Rocha, F.F.; Pires, P.A.; Costa, E.A.; de Matos, L.G.; Kaiser, C.R.; Costa, S.S. Antinociceptive and anti-inflammatory kaempferol glycosides from *Sedum dendroideum*. *J. Ethnopharmacol.* **2009**, *124*, 228–232. [CrossRef]
77. Yildiztugay, E.; Ozfidan-Konakci, C.; Kucukoduk, M.; Turkan, I. Flavonoid Naringenin Alleviates Short-Term Osmotic and Salinity Stresses Through Regulating Photosynthetic Machinery and Chloroplastic Antioxidant Metabolism in *Phaseolus vulgaris*. *Front. Plant Sci.* **2020**, *11*, 682. [CrossRef]

78. An, J.; Kim, S.H.; Bahk, S.; Vuong, U.T.; Nguyen, N.T.; Do, H.L.; Kim, S.H.; Chung, W.S. Naringenin Induces Pathogen Resistance against *Pseudomonas syringae* through the Activation of NPR1 in *Arabidopsis*. *Front. Plant Sci.* **2021**, *12*, 672552. [CrossRef]
79. Girish, T.K.; Kumar, K.A.; Prasada Rao, U.J.S. C-Glycosylated flavonoids from black gram husk: Protection against DNA and erythrocytes from oxidative damage and their cytotoxic effect on HeLa cells. *Toxicol. Rep.* **2016**, *3*, 652–663. [CrossRef]
80. Dai, L.; Hu, Y.; Chen, C.-C.; Ma, L.; Guo, R.-T. Flavonoid C-Glycosyltransferases: Function, Evolutionary Relationship, Catalytic Mechanism and Protein Engineering. *Chem. Bio Eng. Rev.* **2021**, *8*, 15–26. [CrossRef]